Implementing the crossed-sine wavefront sensor for astronomy application with a single natural guide star

Francois Henault, Yan Feng, Jean-Jacques Correia, Alain Spang, Laura Schreiber

Implementing the crossed-sine wavefront sensor for astronomy application with a single natural guide star

François Hénault (a), Yan Feng (a), Jean-Jacques Correia (a), Alain Spang (b), Laura Schreiber (a,c)

(a) Institut de Planétologie et d'Astrophysique de Grenoble, Université Grenoble-Alpes, CNRS, B.P. 53, 38041 Grenoble, France
(b) Université Côte d'Azur, Observatoire de la Côte d'Azur, CNRS, Laboratoire Lagrange, France
(c) INAF, Osservatorio di Astrofisica e Scienza dello Spazio di Bologna, Via Gobetti 93/3, 40129 Bologna, Italy ;

ABSTRACT:

The Crossed-sine Wavefront sensor (CS-WFS) is based on a gradient transmission filter and a 2 x 2 mini-lens array, enabling simultaneous achromatic imaging at a high spatial resolution and measurement accuracy comparable to those of laser-interferometers [1-2]. The imaging system is very compact and can serve a large range of high throughput applications in astronomy, biomedicine and metrology. The performance of the system has been demonstrated recently in the optic laboratory.

However the principle of the crossed-sine WFS is based on simultaneous acquisitions of four off-axis light sources, which may be a limitation when dealing with Adaptive optics (AO) systems for astronomy. This communication presents an alternative design allowing the system to operate with a single, on-axis natural guide star. The new design is described, and numerical simulations confirm that the achieved performance is similar as in the original design.

Keywords: Adaptive Optics, Wavefront sensor; SCAO

1. INTRODUCTION

Wavefront sensors (WFS) have now become core components in the fields of adaptive optics for astronomy [1], biomedical optics [2], and metrology of optical systems [3]. However, it remains challenging to achieve simultaneously high spatial resolution at the pupil of the tested optics and absolute measurement accuracy comparable to that attained by laser-interferometers. In the past years, we developed a new WFS concept that is the Crossed-sine WFS (CS-WFS). Its basic principle and theory was firstly patented in Ref. [4], and later published in Refs. [5-6]. We have recently demonstrated with a prototype that this WFS can achieve both previous goals [7]. The French appellation of this prototype is ASONG, standing for "Analyseur de Surface d'Onde de Nouvelle Génération".

The general measurement configuration of ASONG is illustrated in Figure 1 which consists of the following essential elements:

- An optical measurement head achieving the simultaneous acquisition of four grayscale pupil images;
- A computation unit for the digital reconstruction of the wavefront error (WFE) from the four acquired images, providing a multiplex advantage and reducing noises,
- The optical system to be tested;
- A light source or an illuminated object, emitting or reflecting four off-axis beams through the tested optical system up to the measurement head.

In particular, the optical measurement head comprises two core elements:

- A spatial Gradient transmission filter (GTF) located at the image plane of the tested optics, encoding the Wavefront errors (WFE) into grayscale pupil images,
- A Mini-lens array (MLA) forming the four separated images of the pupil of the testes optics on a detector array.

The need of four different, separated light sources is not critical for bio-optics and laboratory metrology applications. However it may be a limitation when dealing with Adaptive optics (AO) systems for astronomy. This communication presents an alternative design of the CS-WFS allowing the system to be operating with a single, on-axis Natural guide star (NGS). The new design is described in section 2, and numerical simulations in section 3 confirm that the achieved performance is similar to that of the original design. Application of this new LGS CS-WFS to Laser guide stars (LGS) remains to be explored.

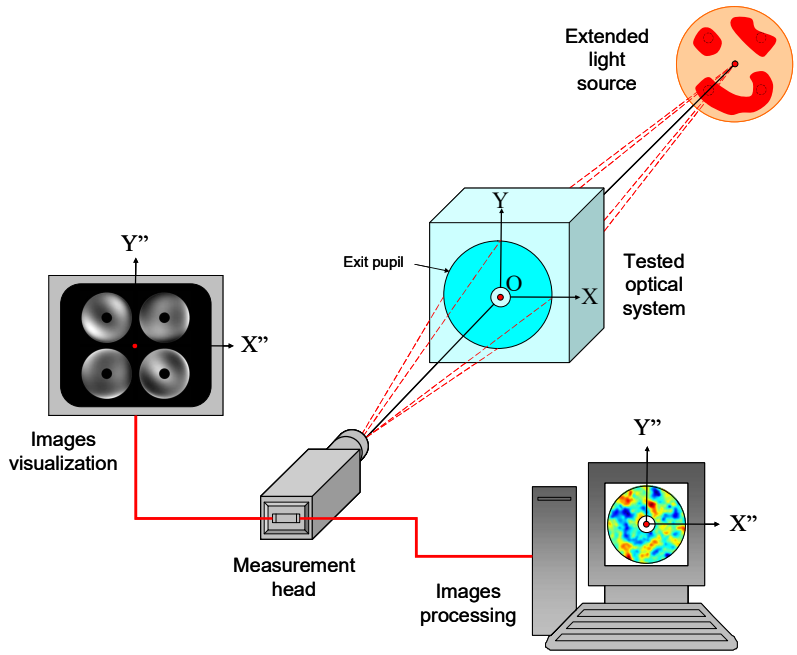

Figure 1: Basic principle of the CS-WFS making use of four off-axis light sources.

2. PRINCIPLE

Adapting the basic principle of the CS-WFS here above described to the case of a single, central NGS for astronomy applications can be achieved by coupling the CS-WFS with the Crossed cubes nuller (CCN). The latter was originally designed for coronagraphy and nulling interferometry applications. Its theoretical analysis was firstly described in Ref. [8] and later demonstrated experimentally in Ref. [9]. It consists in two beam-splitting cubes that are rotated one with respect to the other so that the internal faces of their beam-splitting layers are set perpendicular (see the central part of Figure 2). Three cases may be considered:

- For coronagraphy applications: one single beam impinges the centre of one of the two entrance faces of Cube 1. The beam is then divided into two separated beams, themselves being again divided by two by Cube 2. The four separated output beams are then combined multi-axially by means of a converging lens. A dark central spot is observed at the focus of the lens.

- For NGS wavefront sensing the cubes setup is fully similar, bur there is no need for multi-axial combination since we wish to form four separated images of the telescope pupil on the same detector. Thus the converging lens is removed and replaced with the CS-WFS MLA.

- Lastly, for nulling interferometry applications, the light collected by four telescopes propagates in reverse sense: the four incident beans on Cube 2 are coherently added in the output ports of Cube 1. After being focused, two of them exhibit a central null in the detection plane. However, such use of the CCN is not relevant here.

Returning to the NGS CS-WFS, the final optical configuration is sketched in Figure 2. From left to right and following the sense of light propagation, one can see the input wavefront distorted by atmosphere crossing, the collecting telescope focusing the beam at the entrance of the CCN (Cube 1), and four separated output parallel beams exiting from Cube 2. Afterward follow the Gradient transmission filter (GTF), the Mini-lens array (MLA), and the final detection plane where four side-by-side images of the telescope pupil are sensed. It must be noted that:

- The wavefronts at the exit of Cube 2 have been flipped horizontally, vertically, or both one with respect to the other due to their different geometrical transmissions and reflections at the internal beam-splitting layers.

- Only one monolithic GTF common to the four beams is required, provided that the four output beams of Cube 2 are impinging on identical transmission patterns,

- In Figure 2 the actual distance between the GTF and MLA has been exaggerated for the sake of illustration. In reality they should be as close as possible one to the other, as for the original CS-WFS design.

The conceptual design and performance of the NGS CS-WFS have been tested by way of numerical simulations presented in the next section.

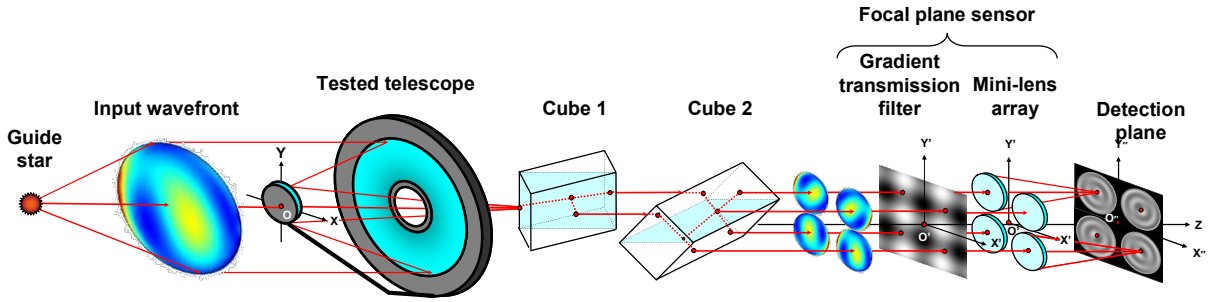

Figure 2: Coupling the CS-WFS with the CCN for a single central light source (NGS). The sizes of the optical elements are not to scale.

3. NUMERICAL SIMULATIONS

Numerical simulations were carried out in order to estimating the net WFE measurement accuracy in terms of Peak-to-Valley (PTV) and RMS numbers. The same numerical model as that described in Ref. [5] is used, assuming that the light source is monochromatic at the wavelength $\lambda = 0.5$ µm. The telescope focal length is equal to $F = 100$ m and its diameter to $D = 10$ m. The recorded image intensities are assumed to be free of noise as in Ref. [5]. Four different cases of distorted WFE were considered. Each case is summarized in Table 1. Care was taken that the simulated cases correspond to the real phase screens implemented on the ASONG test bench as much as possible [7] in view of future performance tests. The PTV and RMS numbers of each input WFE are indicated in Table 2 for each test case. The same numbers for the reconstructed WFEs and their differences with respect to the input WFEs are indicated in Table 2 for each test case. The table also indicates the same metrics for the WFE slopes along the X and Y axes. These results are also illustrated by the false-color views of Figure 3.

The achieved performance shows good WFE measurement accuracy that is about λ/600, λ/110, λ/65 and λ/320 in RMS sense, for the cases Zern 48, Kolmogorov, Residual and Sinus respectively. These numbers are comparable to those obtained with the original SC-WFS design [5]. They could even be improved in two ways:

1) Examining the color maps in Figure 2, one can see that the major measurement errors are located close to the pupil rim for two cases at least (Zernike 48, Sinus). Such areas could be eliminated by use of software pupil masks, at the price of a small reduction of the measurement areas,

2) It can also be expected that these pupil rim effects will be reduced naturally when working in an extended spectral bandwidth.

However the main difference with respect to the original SC-WFS design is that only one single central NGS can be observed, therefore losing the multiplex advantage. Moreover, the CCN optical components are added that will lessen the global WFS transmission. Thus additional numerical simulations are needed to establish a final comparison between both SC-WFS types, and should include the detection noises (shot noise, read-out noise and dark current). This will be the scope of future work.

Table 1: Summary of the simulated phase screens characteristics

Name	Case	Remark
Zernike 48	Atmosphere perturbations, or shape deformations of the mirrors	Medium order Zernike polynomials
Kolmogorov	Aberration introduced by Earth atmosphere	Fried's radius r_0 = 25 mm
Residual	Residual atmospheric aberration after adaptive optics loop correction	First 200 modes corrected
Sinus	Periodic errors of the mirrors generated by an automated polishing machine	Combination of three sine functions of different periods, amplitudes and orientations

Table 2: Results of numerical simulations in terms of PTV and RMS errors for the four considered cases.

	Zernike 48						**Kolmogorov**					
	X-Slopes (µrad)		**Y-Slopes (µrad)**		**WFE (waves)**		**X-Slopes (µrad)**		**Y-Slopes (µrad)**		**WFE (waves)**	
	PTV	RMS	PTV	RMS	PTV	RMS	PTV	RMS	PTV	RMS	PTV	RMS
Reference WFE and slopes	1,970	0,318	1,970	0,318	1,415	0,261	15,384	1,638	15,081	1,689	8,367	1,543
Measured WFE and slopes	1,911	0,313	1,911	0,313	1,412	0,261	13,031	1,623	12,960	1,704	8,215	1,543
Reconstruction errors	1,579	0,005	1,579	0,005	0,047	0,002	12,340	1,077	13,124	1,101	0,872	0,075

	Residual						**Sinus**					
	X-Slopes (µrad)		**Y-Slopes (µrad)**		**WFE (waves)**		**X-Slopes (µrad)**		**Y-Slopes (µrad)**		**WFE (waves)**	
	PTV	RMS	PTV	RMS	PTV	RMS	PTV	RMS	PTV	RMS	PTV	RMS
Reference WFE and slopes	8,854	0,941	8,471	0,951	1,411	0,178	3,633	0,820	3,151	0,771	1,650	0,390
Measured WFE and slopes	6,586	0,952	7,056	0,972	1,400	0,185	3,773	0,805	3,374	0,737	1,637	0,387
Reconstruction errors	6,463	0,643	6,435	0,646	0,207	0,022	2,369	0,066	2,535	0,055	0,116	0,005

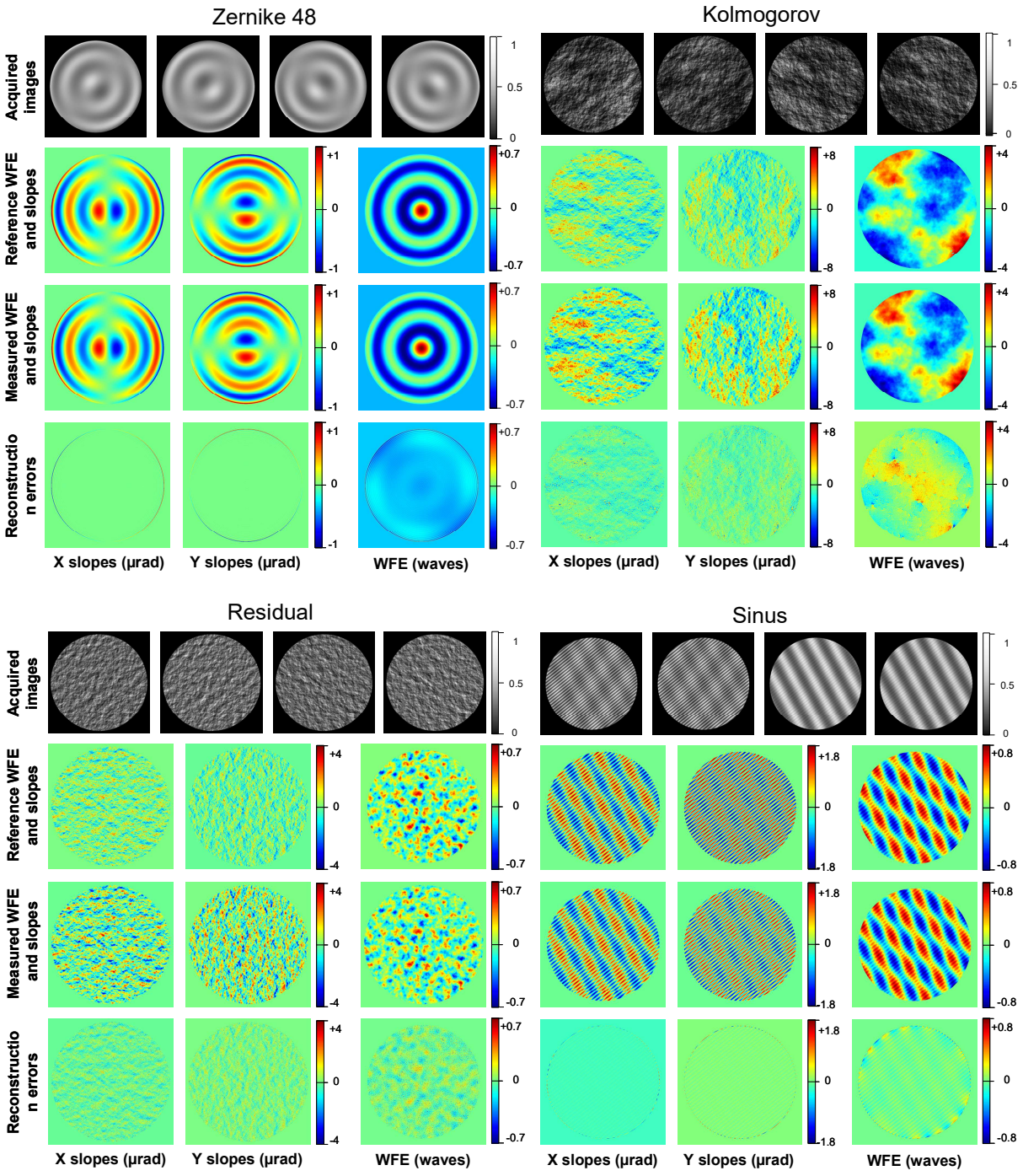

Figure 3: Results of numerical simulations for the four considered cases, illustrated as false-color maps.

4. CONCLUSION

Starting from the original design of the Crossed-sine Wavefront sensor (CS-WFS) that makes uses of four different light sources measured simultaneously, and that was conceived for metrology and ophthalmology applications, this communication presents a variant suitable to astronomy application. It is usable in adaptive optics systems and needs only a single central light source. The new design incorporates a Crossed cubes nuller (CCN) originally intended for coronagraphy and nulling interferometry. After describing the whole system, numerical simulations were carried out in order to demonstrating that it achieves at least as good performance in terms of WFE measurement accuracy as the original CS-WFS concept. These results need to be confirmed when adding detection noises into the numerical model. This will be the scope of future work.

REFERENCES

[1] J. W. Hardy, J. E. Lefebvre, and C. Koliopoulos, “Real-time atmospheric compensation,” JOSA, 67(3), 360-369, (1977).

[2] T. O. Salmon, L. N. Thibos, and A. Bradley, “Comparison of the eye’s wave-front aberration measured psychophysically and with the Shack–Hartmann wave-front sensor,” JOSA A, 15(9), 2457-2465, (1998).

[3] C. R. Forest, C. R. Canizares, D. R. Neal et al., “Metrology of thin transparent optics using Shack-Hartmann wavefront sensing,” Optical engineering, 43(3), 742-754, (2004).

[4] F. Hénault, A. Spang, “Système de contrôle de surfaces d’onde optique par filtre à gradient de densité,” WO2020156867.

[5] F. Hénault, A. Spang, Y. Feng, and L. Schreiber, "Crossed-sine wavefront sensor for adaptive optics, metrology and ophthalmology applications," *Engineering Research Express,* vol. 2, no. 015042, 2020.

[6] Y. Feng, F. Hénault, L. Schreiber, A. Spang, “Development and implementation of crossed-sine wavefront sensor for simultaneous high spatial resolution imaging,” Proceedings of the SPIE vol. 10379, n° 103790N (2020).

[7] L. Schreiber, Y. Feng, A. Spang, F. Hénault, J.-J. Correia, E. Stadler, D. Mouillet, “The crossed-sine wavefront sensor: first tests and results,” Proceedings of the SPIE vol. 12188, n° 121883I (2022).

[8] F. Hénault, A. Spang, “Cheapest nuller in the world: Crossed beamsplitter cubes,” Proceedings of the SPIE vol. 9146, n° 914604 (2014).

[9] F. Hénault, B. Arezki, G. Bourdarot, A. Spang, “Experimental demonstration of a crossed cubes nuller for coronagraphy and interferometry,” Proceedings of the SPIE vol. 9907, n° 99072H (2016).